Infinite-Order Transitions in Density-Functional Models of Wetting

K. Koga,[1] J. O. Indekeu,[2] and B. Widom[3]

[1]Department of Chemistry, Faculty of Science, Okayama University, Okayama 700-8530, Japan
[2]Institute for Theoretical Physics, Katholieke Universiteit Leuven, BE-3001, Leuven, Belgium
[3]Department of Chemistry, Baker Laboratory, Cornell University, Ithaca, New York 14853-1301, USA

(Received 18 November 2009; published 19 January 2010)

A class of density-functional models for wetting transitions is defined. A necessary condition for the transitions to be of higher than first order is derived. A locus of wetting transitions in the plane of two model field variables is determined on which there are states of first-order and of higher-order, including infinite-order, transitions. The observed behavior is rationalized via a different but related, analytically soluble model.

DOI: 10.1103/PhysRevLett.104.036101 PACS numbers: 68.08.Bc, 64.60.−i, 68.35.Rh

In this Letter, we pose and answer the following fundamental questions. What is the global wetting phase diagram for a class of standard density-functional models of three-phase equilibrium with two components? Given that the models possess a minimal number of two parameters, one control parameter b for inducing wetting and one anisotropy parameter a that influences the order of the wetting phase transition, what kinds of wetting transitions are predicted? How robust is the classical second-order wetting transition, found for the symmetric model ($a = 1$), to the introduction of asymmetry ($a \neq 1$)? Furthermore, we uncover a family of infinite-order wetting transitions at the heart of the model, in the symmetric limit ($a \rightarrow 1$), and robust to changes in the control parameter b.

When three phases are in equilibrium it may be that one ''wets'' (spreads at) the interface between the other two, or, alternatively, they may meet along a line of common contact of all three with three nonvanishing contact angles. The transition between those two modes of three-phase equilibrium is termed a wetting transition. It has been the subject of much interest and of many reviews, as in Refs. [1–7]. Here we study, partly analytically and partly numerically, a class of mean-field density-functional models with wetting transitions, both of the first and of higher than first order. We determine in the context of the models the conditions that govern the order of the transition and the exponents that characterize the thermodynamic singularities at the transition.

The model free-energy densities Ψ in this study are of the form

$$\Psi = F[\rho_1(z), \rho_2(z); a, b] + \tfrac{1}{2}[\rho_1'(z)^2 + \rho_2'(z)^2], \qquad (1)$$

where $\rho_1(z)$ and $\rho_2(z)$ are two densities that vary in the direction z perpendicular to an assumed planar interface and a and b are two thermodynamic field variables. For every a and b under consideration, the function F has a common minimum value of 0 when ρ_1, ρ_2 are the densities in the interiors of the three coexisting phases α, β, and γ, at $z = \pm\infty$:

$$\begin{aligned} &\alpha\text{: } \rho_1 = -1, \rho_2 = 0; \\ &\beta\text{: } \rho_1 = 0, \rho_2 = b; \\ &\gamma\text{: } \rho_1 = 1, \rho_2 = 0. \end{aligned} \qquad (2)$$

The tensions $\sigma_{\alpha\beta}$, etc., of the three interfaces are obtained by minimizing the functional

$$\sigma = \int_{-\infty}^{\infty} \Psi dz \qquad (3)$$

with respect to variations in $\rho_1(z)$ and $\rho_2(z)$, subject to the boundary conditions (2) at $z = \pm\infty$. The Euler-Lagrange equations for the $\rho_1(z)$ and $\rho_2(z)$ that minimize the functional in (3) are

$$\partial F/\partial\rho_1 = d^2\rho_1/dz^2, \qquad \partial F/\partial\rho_2 = d^2\rho_2/dz^2, \qquad (4)$$

to be solved subject to those boundary conditions.

We contemplate the wetting or nonwetting of the $\alpha\gamma$ interface by the β phase. Figure 1 shows schematically the solutions of (4) in these circumstances. Figures 1(a) and 1(b) show $\rho_1(z)$ and $\rho_2(z)$ in the $\alpha\beta$ interface with the bulk α phase at $z = -\infty$ and the β phase at $z = +\infty$. The $\beta\gamma$ interface is similar, but with the boundary conditions in (2) for γ replacing those for α. Figures 1(c) and 1(d) are for the $\alpha\gamma$ interface when it is not wet by the β phase, while Figs. 1(e) and 1(f) are for the $\alpha\gamma$ interface when it is wet by β. In Fig. 1(d), showing $\rho_2(z)$ in the nonwet $\alpha\gamma$ interface, ρ_2 reaches a maximum value b_0 that is less than its value b in the bulk β phase. The dashed lines in the interior of the $\alpha\gamma$ interface, at $\rho_1 = 0$ in Fig. 1(e) and at $\rho_2 = b$ in Fig. 1(f), indicate the infinite (i.e., macroscopic) thickness of the β layer intruding in that interface when it is wet by β.

When none of the interfaces between pairs of phases is wet by the third phase, the three interfacial tensions satisfy triangle inequalities of the form below; when the $\alpha\gamma$ interface is wet by β, they satisfy the equality:

$$\begin{aligned} \text{nonwet}: &\ \sigma_{\alpha\gamma} < \sigma_{\alpha\beta} + \sigma_{\beta\gamma}; \\ \text{wet}: &\ \sigma_{\alpha\gamma} = \sigma_{\alpha\beta} + \sigma_{\beta\gamma}. \end{aligned} \qquad (5)$$

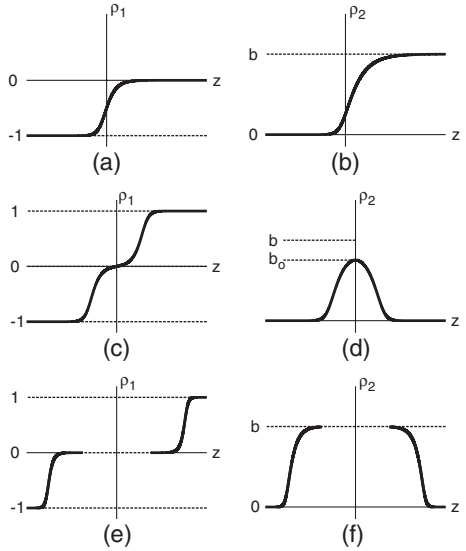

FIG. 1. (a), (b) $\rho_1(z)$ and $\rho_2(z)$ in the $\alpha\beta$ interface. (c), (d) $\rho_1(z)$ and $\rho_2(z)$ in the nonwet $\alpha\gamma$ interface. (e), (f) $\rho_1(z)$ and $\rho_2(z)$ in the $\alpha\gamma$ interface wet by β.

The transition between these two modes is the wetting transition. Our concern is with how $\sigma_{\alpha\beta} + \sigma_{\beta\gamma} - \sigma_{\alpha\gamma}$ vanishes as the parameter b approaches its value b_w at the wetting transition, where b_w is then itself a function of the parameter a. There will be a one-dimensional manifold of wetting-transition points in the a, b plane. At the first-order wetting transitions, $\sigma_{\alpha\beta} + \sigma_{\beta\gamma} - \sigma_{\alpha\gamma}$ vanishes proportionally to the first power of the distance from the transition locus in the a, b plane; at the higher-order transitions, it vanishes with a greater than first power or exponentially rapidly for an infinite-order transition.

In the immediate neighborhood of the bulk β phase, where $\rho_1 = 0$ and $\rho_2 = b$, our model $F(\rho_1, \rho_2; a, b)$ will take the form

$$F(\rho_1, \rho_2; a, b) = (\rho_1/a_1)^2 + [(b - \rho_2)/a_2]^2, \quad (6)$$

where the anisotropy parameter is now $a = a_1/a_2$. Contours of constant F in the ρ_1, ρ_2 plane in the neighborhood of that point, for fixed a and b, are then ellipses with semiaxes $a_1\sqrt{F}$ and $a_2\sqrt{F}$ in the directions of the ρ_1 and ρ_2 axes, respectively. In what follows, it will be seen that it is the parameter a that determines the character of the wetting transition.

The field variable b typically depends on temperature, chemical potentials, external fields, or some combination of these, and it acts as a control parameter that can induce wetting through changes in these external influences. The variable a is typically associated with the ratio of two competing length scales [8]. The length scales govern the spatial approach of the densities ρ_1 and ρ_2 toward their values in a bulk phase, and the ratio reflects an asymmetry ($a = 1$ for the symmetric case) which is generally independent of temperature but may depend on, for example, uniaxial anisotropy (for magnets) [9] or the Ginzburg-Landau parameter (for superconductors) [10]. These two examples outside the field of fluids illustrate the wide applicability of the class of models we discuss. As regards fluids, we assume short-range interactions. van der Waals forces, which can affect wetting behavior qualitatively [3,4,7], are not allowed for.

Figure 2 shows schematically, as trajectories in the ρ_1, ρ_2 plane, how ρ_1 and ρ_2 vary together through the three interfaces. They are obtained in principle by eliminating z from $\rho_1(z)$ and $\rho_2(z)$, thus obtaining ρ_2 as a function of ρ_1. The solid curve in the figure is a composite of the $\alpha\beta$ and $\beta\gamma$ interfaces and is then also the corresponding trajectory for the $\alpha\gamma$ interface when it is wet by β. The dashed curve is for the $\alpha\gamma$ interface when it is not wet by β. On this nonwetting trajectory, ρ_2 reaches a maximum at $b_0 < b$, as in Fig. 1(d). While $b > b_w$, the tension $\sigma_{\alpha\gamma}$ associated with the nonwetting trajectory is less than the sum $\sigma_{\alpha\beta} + \sigma_{\beta\gamma}$ associated with the composite wetting trajectory, but they become equal at $b = b_w$. For a first-order transition, the equality is achieved while the wetting and nonwetting trajectories are still distinct, so the structure of the $\alpha\gamma$ interface is discontinuous at the transition. At a higher-order wetting transition, by contrast, the equality (5) is achieved only when the dashed curve in Fig. 2 has become identical with the solid curve. The structure of the $\alpha\gamma$ interface is then continuous at the transition.

From Eqs. (4) and their first integral $F = (1/2) \times [\rho_1'(z)^2 + \rho_2'(z)^2]$, one finds the ρ_1, ρ_2 trajectories in Fig. 2 to satisfy the differential equation

$$F\frac{d^2\rho_2}{d\rho_1^2} = \frac{1}{2}\left[1 + \left(\frac{d\rho_2}{d\rho_1}\right)^2\right]\left(\frac{\partial F}{\partial \rho_2} - \frac{\partial F}{\partial \rho_1}\frac{d\rho_2}{d\rho_1}\right). \quad (7)$$

One consequence of (7) is that in the neighborhood of each of the three bulk-phase points in the ρ_1, ρ_2 plane, where the contours of constant F are elliptical, the trajectory on entering or departing that point must do so tangentially to the long axes of the ellipses. Thus, in the example of Fig. 2, the long axes at all three bulk-phase points have been supposed horizontal. In particular, for the β-phase point $\rho_1 = 0$, $\rho_2 = b$ in Fig. 2, this means we were implicitly taking the a_1 and a_2 in (6) to be such that $a_1/a_2 > 1$. A

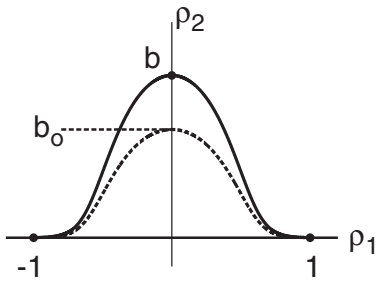

FIG. 2. $\alpha\gamma$ interfacial trajectories in the ρ_1, ρ_2 plane. Solid curve wetting and dashed curve nonwetting. Phase α at $\rho_1 = -1$, $\rho_2 = 0$; phase β at $\rho_1 = 0$, $\rho_2 = b$; phase γ at $\rho_1 = 1$, $\rho_2 = 0$.

second, related consequence of (7) is that on the wetting trajectory, near the β phase, if $a_1/a_2 < 2$, then

$$b - \rho_2 = A|\rho_1|^{a_1/a_2} \tag{8}$$

with A a positive proportionality factor. When $a_1/a_2 > 2$, the leading exponent in (8) remains 2; thus, $b - \rho_2 = A'{\rho_1}^2$. But in this case, the coefficient A' is itself proportional to the coefficient of the further term $(b - \rho_2){\rho_1}^2$ in the expansion of F about $b - \rho_2 = 0$, $\rho_1 = 0$; so if, by some special symmetry of F, that term is absent in the expansion, the exponent of the leading term in (8) reverts to a_1/a_2 even when $a_1/a_2 > 2$.

The third consequence of (7) we wish to note here is that on the nonwetting trajectory in Fig. 2, which passes through the point $\rho_1 = 0$, $\rho_2 = b_0 < b$, we have near that point,

$$b_0 - \rho_2 \sim \frac{1}{2(b - b_0)}{\rho_1}^2. \tag{9}$$

If the wetting transition is of higher order, then, as remarked earlier, the two trajectories in Fig. 2 become identical at the transition; so, in particular, $b_0 \to b(\to b_w)$. But (9) says that the second derivative of ρ_2 with respect to ρ_1 on the nonwetting trajectory diverges as $b_0 \to b$. Then from this property of the nonwetting trajectory, and from (8) for the wetting trajectory, we have $a_1/a_2 < 2$ as a necessary condition for the transition to be of higher order. Therefore, $a_1/a_2 \geq 2$ is equally well a sufficient condition for the transition to be of first order. In one of the models studied earlier [11,12], $a_1/a_2 = \sqrt{3}/b$ and $b_w = 0.510\cdots$, so $a_1/a_2 > 2$ at the transition. For that model, $b - \rho_2$ vanishes proportionally to ${\rho_1}^2$ on the wetting trajectory, as expected, but since the exponent is still not less than 2, the transition must be of first order, as it was found to be, in agreement with the principle enunciated above. In another model studied earlier [13], $a_1/a_2 = 1$, so it satisfies the necessary condition for a higher-order transition and was indeed found to be a classical second-order transition, again consistently with the principle. We will have $a_1/a_2 < 2$ (in fact, we will have $a_1/a_2 \leq 1$) at all the higher-order transitions that occur in the models studied here.

For the class of models treated here the $F(\rho_1, \rho_2; a, b)$ in (1) is taken to be a standard triple-well potential

$$F(\rho_1, \rho_2; a, b) = [(\rho_1 + 1)^2 + {\rho_2}^2][(\rho_1 - 1)^2 + {\rho_2}^2] \times [(\rho_1/a)^2 + (\rho_2 - b)^2], \tag{10}$$

for which, indeed, $a_1/a_2 = a$.

From the numerical analysis described below, we find the locus of wetting-transition points in the a, b plane to be as shown in Fig. 3. In states a, b above and to the left of the transition locus, the $\alpha\gamma$ interface is not wet by β; in states a, b below and to the right, the $\alpha\gamma$ interface is wet by β. The vertical segment in the transition locus at $a = 1$ extends from $b = 0$ to $b = \sqrt{2\sqrt{3} - 3} = 0.681\cdots$ [13],

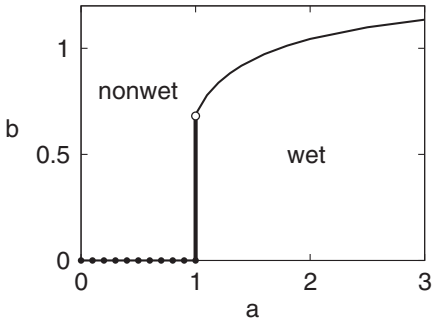

FIG. 3. Locus of wetting transitions in the a, b plane. On the horizontal segment (line with dots) at $b = 0$, $0 < a < 1$, the transition is of higher than first order; on the vertical segment (thick line) at $a = 1$, $0 < b < \sqrt{2\sqrt{3} - 3} = 0.681\cdots \equiv b_{w2}$, it is of infinite order; on the solid curve at $a > 1$, it is of first order. In states above and to the left of the transition locus, the $\alpha\gamma$ interface is not wet by β; on states below and to the right of it, the $\alpha\gamma$ interface is wet by β.

which will be denoted b_{w2}. This point $a = 1$, $b = b_{w2}$ is where the wetting transition changes from higher than first order when $a \leq 1$ and $b \leq b_{w2}$ to first order when $a > 1$ and $b > b_{w2}$.

The earlier study [13], referred to above, was for the special case of (10) in which $a = 1$. It was found there that as $b \to b_w = b_{w2}$ from above, $\sigma_{\alpha\beta} + \sigma_{\beta\gamma} - \sigma_{\alpha\gamma}$ vanishes proportionally to $(b - b_w)^2$, so it is then a classical second-order transition. For $0 < a < 1$ the wetting transition as found here numerically occurs when $b \to 0$ and is found to be of higher order with $\sigma_{\alpha\beta} + \sigma_{\beta\gamma} - \sigma_{\alpha\gamma}$ vanishing proportionally to $b^{2/(1-a)}$. We note that the exponent is not universal but depends on the parameter a. Further, we find that when any point $a = 1$, $b < b_{w2}$ on the vertical segment of the wetting-transition locus is approached as $a \to 1$ from below with b fixed, $\sigma_{\alpha\beta} + \sigma_{\beta\gamma} - \sigma_{\alpha\gamma}$ then vanishes proportionally to $\exp[-c/(1 - a)]$ with a positive constant c, so these wetting transitions are all of infinite order.

We note that the necessary condition $a_1/a_2 < 2$ for the transition to be of higher than first order is satisfied here for all of these cases we have so far referred to in which $a \leq 1$. For the range $1 < a < 2$, the condition allows but does not require the transitions to be of higher than first order, and we find them in fact to be of first order, although we do not know of any general criterion that required it. For $a \geq 2$, the criterion requires the transitions to be of first order, as we find them to be.

Following a brief description of the numerical procedures that led to this picture, we introduce a different but related, analytically soluble model with which we are able to rationalize these results of the numerical calculations.

The densities $\rho_1(z)$ and $\rho_2(z)$ for each interface are obtained by numerically solving (4) subject to the boundary conditions (2). The differential equations are approximated by five-point difference equations on a uniform grid in z and then solved iteratively with a successive over-

relaxation method. The range of z is taken to be $[-10, 10]$, $[-20, 20]$, or $[-40, 40]$ and is discretized with a grid spacing of 0.01. The criterion for convergence is a rms difference of less than 1×10^{-14} between iterates. The surface tensions $\sigma_{\alpha\beta}(=\sigma_{\beta\gamma})$ and $\sigma_{\alpha\gamma}$ are then obtained, via (3), as functions of b with a fixed in a range $0 < a < 3$ or as functions of a with b fixed. We note that the calculation of $\sigma_{\alpha\gamma}$ becomes increasingly difficult as b goes to b_w or as a goes to 1 on approach to the locus of continuous wetting transitions. The lower limit of b or the upper limit of a is taken to be that where the calculation of $\sigma_{\alpha\gamma}$ completes typically within 24 hours with an eight-core 3 GHz Intel Xeon processor.

Now we introduce an analytically soluble model. This model, too, has a free-energy density Ψ of the form (1) with the function F as described below it. As in the density-functional models studied above, $\rho_1(z)$ and $\rho_2(z)$ of the $\alpha\beta$ and $\beta\gamma$ interfaces are those which minimize $\int \Psi dz$, or equivalently the solutions of (4), subject to the boundary conditions (2). When the densities are close to those in the bulk β phase at $z = +\infty$ and b is close to 0, one finds

$$|\rho_1(z)| = k_1 e^{-z/a_1}, \qquad b - \rho_2(z) = k_2 b e^{-z/a_2}, \quad (11)$$

where k_1, k_2 are some positive constants. Eliminating z from (11) results in the wetting trajectory of the form (8). The coefficient A in (8) is thus identified as $k_2 b/{k_1}^a$, where $a = a_1/a_2$. It is now supposed that, in the ρ_1, ρ_2 plane, the nonwetting trajectory differs from the wetting trajectory only in some small range of $|\rho_1| < \rho_1^*$ where F is of the form (6): it is taken to intersect the wetting trajectory at $|\rho_1| = \rho_1^*$ and to become identical to it for $\rho_1^* < |\rho_1| < 1$. These suppositions are not true of the original model, so we have now in effect defined a different, but clearly related, model. Now the density profiles $\rho_1(z)$ and $\rho_2(z)$ for the nonwetting interface, too, consist of two parts, of which the one corresponding to the trajectory in the range $|\rho_1| < \rho_1^*$ is obtained as analytical solutions of (4) subject to the boundary conditions $\rho_1 = 0$, $\rho_2 = b_0 < b$ and $|\rho_1| = \rho_1^*$, $\rho_2 = b - A\rho_1^{*a}$. The surface tension $\sigma_{\alpha\gamma}$ is then obtained by minimizing (3) with respect to the variation in the intersection point ρ_1^*. The final result for $a < 1$ is

$$\sigma_{\alpha\beta} + \sigma_{\beta\gamma} - \sigma_{\alpha\gamma} = \frac{k_1^2(1-a^2)}{a_2 a^2}\left[\frac{k_2}{k_1}\frac{a}{a+1}b\right]^{2/(1-a)}. \quad (12)$$

The right-hand side is greater than 0 as required; it vanishes proportionally to $b^{2/(1-a)}$ as $b \to 0$ for fixed a and vanishes exponentially rapidly as a goes to 1 from below for fixed $b < 2k_1/k_2$. These analytical results are in excellent agreement with, and may be taken to explain, the numerical results for the density-functional models with $0 < a < 1$ including the limit of $a \to 1$ from below. Our calculation here is in the same spirit as in previous interface potential approaches for two-component order parameters [8–10].

In conclusion, we have shown that the classical second-order wetting transition found for a standard density-functional model ($a = 1$) is notably sensitive to any perturbation that introduces an asymmetry in the characteristic length scales of the spatial variation of the two order parameters. For $a > 1$ classical first-order transitions are predicted. For $a < 1$ nonuniversal critical wetting transitions are found, with critical exponents that vary continuously with a. This is reminiscent of the wetting transition at a wall studied by asymmetric two-component mean-field models [8] and by a nonlocal interface Hamiltonian theory which fully captures the effects of thermal fluctuations [14]. Beside these wetting transitions, a family of infinite-order wetting transitions emerge as a function of the asymmetry parameter in the symmetric limit ($a \to 1$). For the infinite-order transitions to occur, no special tuning of the control parameter b is needed, while for all of the other first-order, second-order, and nonuniversal critical wetting transitions, b must be tuned to a specific value $b_w(a)$ that depends on a. In sum, infinite-order transitions take a central rather than peripheral place among wetting transitions.

The authors acknowledge support from a Grant-in-Aid for Scientific Research and the Next Generation Super Computing Project from MEXT, Japan (K. K.), from Grant No. G.0115.06, FWO-Vlaanderen (J. O. I.), and from the U.S. National Science Foundation (B. W.).

[1] H. Nakanishi and M. E. Fisher, Phys. Rev. Lett. **49**, 1565 (1982).
[2] J. S. Rowlinson and B. Widom, *Molecular Theory of Capillarity* (Oxford University Press, New York, 1982), Section 8.5.
[3] P. G. de Gennes, Rev. Mod. Phys. **57**, 827 (1985).
[4] S. Dietrich, in *Phase Transitions and Critical Phenomena*, edited by C. Domb and J. L. Lebowitz (Academic Press, New York, 1988), Vol. 12, Chap. 1.
[5] M. Schick, in *Liquides aux Interfaces/Liquids at Interfaces*, Les Houches, Session XLVIII, edited by J. Charvolin, J. F. Joanny, and J. Zinn-Justin (Elsevier, New York, 1990).
[6] J. Kuipers and E. M. Blokhuis, J. Chem. Phys. **131**, 044702 (2009).
[7] D. Bonn, J. Eggers, J. Indekeu, J. Meunier, and E. Rolley, Rev. Mod. Phys. **81**, 739 (2009).
[8] E. H. Hauge, Phys. Rev. B **33**, 3322 (1986).
[9] C. J. Walden, B. L. Györffy, and A. O. Parry, Phys. Rev. B **42**, 798 (1990).
[10] J. M. J. van Leeuwen and E. H. Hauge, J. Stat. Phys. **87**, 1335 (1997).
[11] I. Szleifer and B. Widom, Mol. Phys. **75**, 925 (1992).
[12] K. Koga and B. Widom, J. Chem. Phys. **127**, 064704 (2007).
[13] K. Koga and B. Widom, J. Chem. Phys. **128**, 114716 (2008).
[14] N. R. Bernardino, A. O. Parry, C. Rascón, and J. M. Romero-Enrique, J. Phys. Condens. Matter **21**, 465105 (2009).